

The C.E.V. injector ion source

L. Ah-Hot, J. Arianer, J. Baixas, P. Debray, M. Malard, and A. Serafini
Institut de Physique Nucléaire, Orsay, France

Presented by P. Debray

ABSTRACT

The multicharge heavy ion source attached to the cyclotron injector is of the hot-cathode reflex type. The high power arc is pulsed in order to produce highly charged states. The ion source, electric focusing, and magnetic analysing elements are mounted on a platform brought to a 140 kV d.c. voltage. Qualitative and quantitative results are presented.

1. INTRODUCTION

Preliminary design of the ALICE machine was limited to Ar^{4+} ions. The first ion source model was tested in our laboratory and consisted of a heated cathode ion source, located in the axis of an air-cored magnet producing a 1.5 kG field. The beam was extracted radially, between the coils and focused before analysis by a 40° magnet. Ions of N, Ar, Kr, and Xe were analysed.¹⁻²

Developments in multicharge ion sources³ made the acceleration of Kr possible in the Linac, but the first model became obsolete and we had to keep the same ion source as the one working on the cyclotron.

In the second model, the source magnetic field is provided by a C-shaped magnet with a 15 cm gap allowing enough space for an efficient focusing system. Behind the analysing magnet, a second lens has the double function of acceleration and adjustment of the beam to Linac conditions.

These elements are working on a 140 kV isolated platform. The pumping system only is grounded and connected through large diameter Pyrex glass tubes.

2. DESCRIPTION OF THE EXPERIMENTAL MODEL

The ion source in its C-shaped magnet is shown in Fig. 1.

The cathode and filament are made of tungsten, and the reflecting cathode of tungsten or molybdenum. The water-cooled copper anode is at the platform potential. The beam is extracted through a circular slot of 2 or 3 mm in

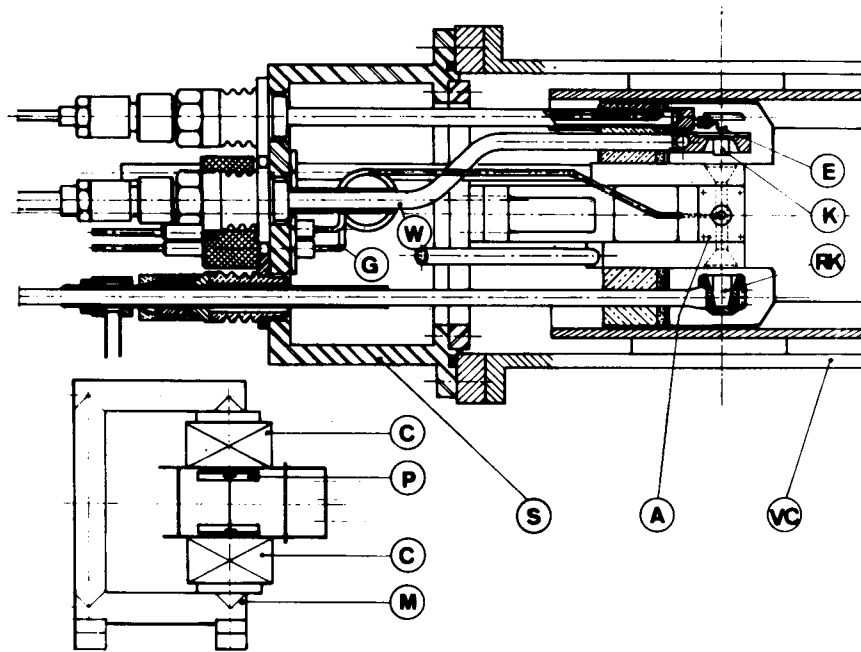


Fig. 1. Ion source section, and source magnet. C—coils, P—magnet poles, M—C-shaped magnet, S—ion source support, E—tungsten filament, K—tungsten cathode, RK—reflecting cathode, A—anode, VC—vacuum chamber, G—gas, W—water,

diameter. The source insulators are made of alumina or steatite. The maximum source magnetic field is 2 kG for 3.2 kW electrical power.

Fig. 2(a) shows the puller with 20 kV extracting voltage, located 3 mm from the source slot.

The first test consisted in observing the beam impact marks on a thin tantalum target. The diameter of the marks was about 10 mm over a 70 mm distance. This measurement gave a first estimation of the beam spread given by the ion source: in this case about 300 mm mrad for 20 kV extracting voltage and 4 mA beam intensity. We had to design a first focusing system using a symmetrical electrical lens.

The ion source magnetic field configuration has to fulfill the following conditions:

- (a) weak constriction on the source axis;
- (b) maximum reduction of the fringing field of the magnet

To obtain these results, the magnetic poles have the shape illustrated by Fig. 2(b). The pole-edges produce the constriction effect. The front pole edge is thicker than the other to compensate for the magnetic influence of the central lens electrode (of iron) to give a strong reduction of the fringing field.

Between source and lens, the magnetic field is still important and we had to adjust the ion source location and rotation to direct the beam into the theoretical trajectory.

Fig. 3 shows this configuration up to the analysing system. Moving targets C1 or C2 allow measurement and observation of the beam.

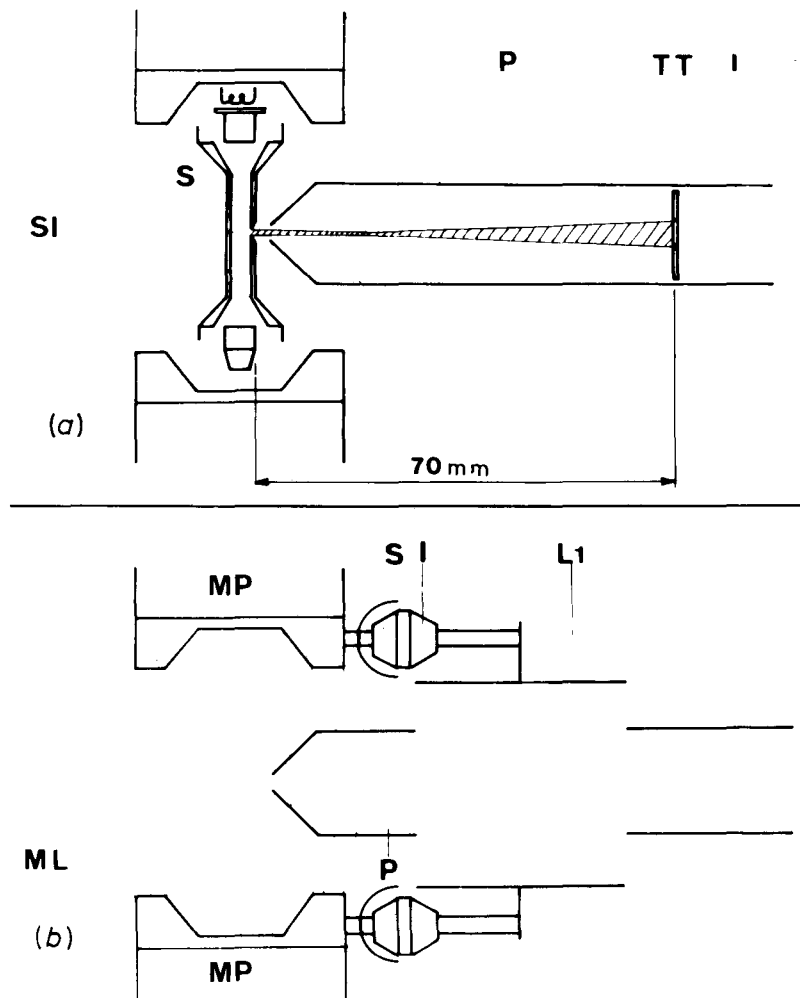


Fig. 2(a). Initial beam path. S—ion source, SL—2 mm diam. hole, P—puller, TT—tantalum target, I—beam impact area. (b) Magnetic field configuration. P—magnet poles, ML—magnetic field lines, P—puller, LI—first electrostatic lens, I—insulator, S—insulator shielding

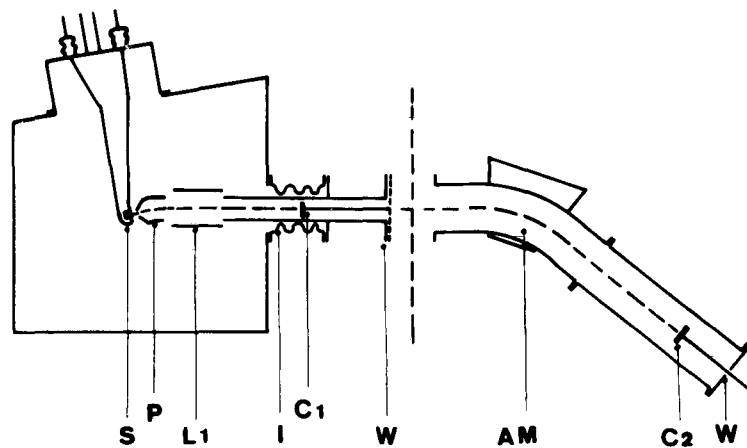


Fig. 3. Geometry of analysing magnet. C1—first target, AM—analysing magnet, C2—second target, W—window, I—extraction voltage insulator

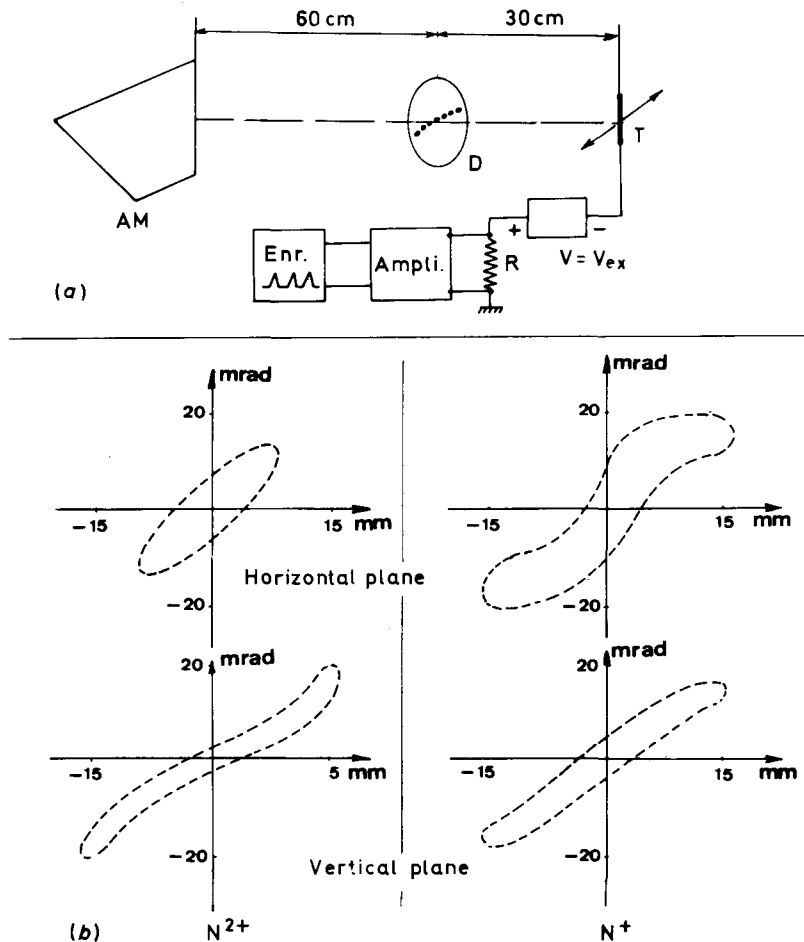


Fig. 4. Emittance measurements. AM—analysing magnet, D—emittance disc, T—moving target

3. MODEL MEASUREMENTS

Model measurements were made in two steps.

3.1. Measurements after L1 lens

The beam was observed on the moving target C1 (Fig. 3) in order to verify the correct beam alignment on the axis. The charge states were separated by the ion source fringing field and we could see clearly the separated impacts of the charges 1–2 for N and Ne, 1–2–3 for Ar, and 1–2–3–4 for Kr.

3.2. Measurements after the analysing magnet

The target C2 is located at a distance of 30 cm from the pole edge of the analysing magnet. With d.c. arc conditions, ion intensities were collected as shown in Table 1.

484

Table 1

<i>Particle</i>	<i>Arc</i>	<i>V_{ex}</i> (kV)	<i>V_{L1}</i> (kV)	<i>I_{C2}</i> (μA)
N ⁺	300 V 2.6 A	18	1.5	800
N ²⁺	390 V 3.8 A	20.6	1.8	450
*N ²⁺	400 V 3.4 A	20	1.7	800
Ne ⁺	300 V 3.6 A	15.5	1.1	160
Ne ²⁺	250 V 4 A	20	1.8	180

* These measurements were made with a source hole of 3 mm instead of 2 mm in diam.

3.3. Emittance

The system is shown in Fig. 4(a). The disc D is radially drilled by holes 1 mm in diam. A collecting wire 30 cm away from the disc moves slowly and intercepts the beam. Measurements were made in both planes and we obtained emittance figures for the ions N⁺ and N²⁺ as shown in Fig. 4(b).

Normalised emittances E_n are given in Table 2.

Table 2

<i>Particle</i>	<i>E_n vertical</i> 10 ⁻⁷ m rad	<i>E_n horizontal</i> 10 ⁻⁷ m rad	<i>I</i> mA
N ⁺	1.2	1.46	1.5
N ²⁺	1.3	1.3	0.8

The results show that the emittances in this case do not vary significantly with the charge state and verify that the figure of 300 mm mrad found behind the ion source is a maximum since the highest value in this table is 270 mm mrad. These model studies also enabled the choice to be made of the lens necessary to give the correct injection velocity.

4. OPTIC CALCULATIONS

Calculations of the trajectories in the electrostatic lenses were made analytically by the Runge-Kutta method. We assume that the potential distribution of a focusing system is obtained by the linear superposition of the potentials

produced by each element of the system. These potentials being expressed in terms of tanh or of Arc tan, the electric fields at each point are given by the series expansion of the potential on the axis:

$$\vec{E}_r(r, z) = -\frac{\partial\phi(r, z)}{\partial r} \quad \vec{E}_z(r, z) = -\frac{\partial\phi(r, z)}{\partial z}$$

with

$$\phi(r, z) = \sum_{k=0}^{\infty} \frac{(-1)^k}{(k!)^2} \left(\frac{r}{2}\right)^{2k} \frac{d^{(2k)}}{dz} \phi(0, z)$$

For a given lens geometry, the trajectories define the transfer matrix of this lens:

$$M = \begin{pmatrix} m_{11} & m_{12} \\ m_{21} & m_{22} \end{pmatrix}$$

and its focal length:

$$F_z = -\frac{m_{11}}{m_{21}}$$

In this manner, we can determine the number of lenses required and their appropriate location. The transition between extraction and injection potential

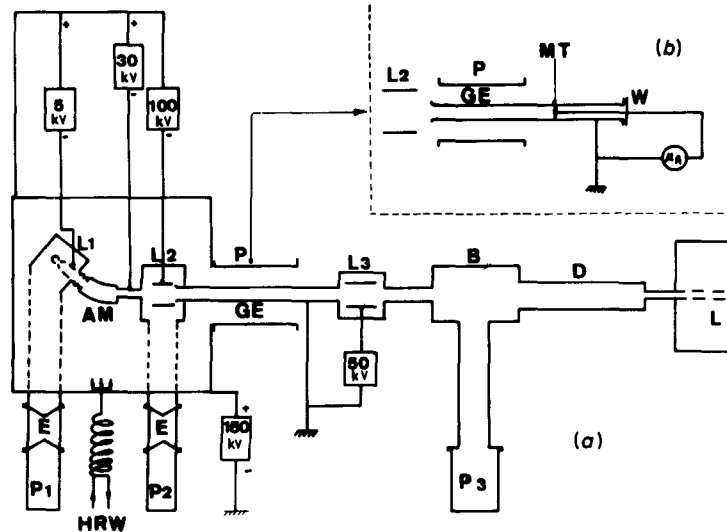


Fig. 5. Schematic diagram of Linac injector. P—injector voltage insulator, GE—ground electrode, L3—third electrostatic lens, B—buncher, D—beam deflecting plates, L—linear accelerator, MT—moving target, W—window, P1—2000 l/s diff. pump, P2—3000 l/s diff. pump, P3—6000 l/s diff. pump, E—striking electrodes, HRW—high resistivity-water choke

requires a particular lens structure in which the potential penetration must be as weak as possible to avoid an overfocusing effect. The acceleration produces at the same time a reduction of the emittance value by the ratio:

$$(V_{ex}/V_{inj})^{1/2}.$$

5. TESTS WITH THE LINAC

Fig. 5(a) shows the ion source connected to the injector.

A second platform contains the ion source power supplies. Electrical information is transmitted to the control-room by light pipes (infra-red for ion source parameters). The first experiments were made with N^{2+} and we obtained the results in Table 3.

Table 3

Ion	Arc	Duty-cycle (%)	Vex (kV)	V _{L1} (kV)	V _{L2} (kV)	V _{L3} (kV)	V _{inj.} (kV)	I _{C2} (μA)
N ²⁺	d.c. 320 V 4 A	100	21	2.25	40	20.5	92	32
N ²⁺	Pulsed 700 V 10 A	20	21	2.25	40	20.5	92	6

The ion source life-time is of the order of 20 h. In pulsed operation, the rise time of the arc current is 50 μs.

A sparking problem occurred in the isolating vacuum tubes of P1 and P2 above 50 kV injection voltage. A solution consisted in providing on each side of the tube, a cone-shaped electrode modifying the potential distribution and giving the maximum electric field along the axis of the tube.

The collected currents on C2 are weaker than the currents obtained with the model. In particular, the intensity falls when the injection voltage is increased.

A target MT is now located behind the injection voltage insulator [Fig. 5(b)] and the following intensities are collected:

$$\begin{aligned} N^+ &- 1 \text{ mA} \\ N^{2+} &- 200 \text{ } \mu\text{A} \end{aligned} \quad \text{for 80 kV injection voltage}$$

As the injection voltage reaches 92 kV (acceleration value for N^{2+}) the intensity falls quickly and confirms the previous results. We conclude that there is a defect in the shape of the lens L2 and particularly in the location and efficiency of its grid (overfocusing effect). Attempts are being made to find a good geometry.

REFERENCES

1. Arianer, J. and Debray, P., *J. de physique* 4, 177, (June 1969).
2. Arianer, J., *Thèse ingénieur CNAM*, (1969).
3. Passiuk, *Preprints J.I.N.R.*, Dubna, 1522-1523, 1644.